Theoretical simulation of beam-foil decay curves for resonance transitions of heavy ions

S. M. Younger and W. L. Wiese
Institute for Basic Standards, National Bureau of Standards, Washington, D.C. 20234
(Received 11 October 1977)

A systematic study of the influence of cascades on heavy-ion beam-foil decay curves has been made. Using theoretical data for the lifetimes and initial populations of excited states, decay curves simulating beam-foil excitation conditions have been constructed for the resonance transition of three ions in the copper isoelectronic sequence. Various models for the initial population distribution were tested by comparison with a detailed beam-foil decay curve available for Kr VIII. We found that customary exponential-fitting methods were not able to extract the primary lifetimes from the simulated curves used in constructing them, although the replenishment ratios were close to zero. General implications of this subtle masking of the primary lifetime by numerous cascades for the accuracy of experimental beam-foil data are discussed, especially for $\Delta n = 0$ transitions in heavy ions.

I. INTRODUCTION

A number of experimental techniques have been developed in recent years to determine atomic lifetimes. These may be grouped into two categories according to the mode of excitation: those that use selective and those that use nonselective excitation. The first type of lifetime experiment, which in practice depends usually on excitation by resonance radiation, is quite restricted in the range of atomic levels to which it may be applied. The second type, in which the excitation is nonselective, is more general and can—at least in principle—be used to obtain the lifetime of any atomic state. A serious problem arising from this generalized excitation scheme, however, is the likelihood of the lengthening of lifetimes by repopulation or "cascading" from higher-lying atomic levels. Cascading has been recognized as a major source of systematic error in such experiments, and various correction and analysis schemes have been developed and applied, starting with the early literature, such as the lifetime work by Heron *et al.*[1]

When the now-dominant beam-foil spectroscopy technique was developed and lifetime measurements became numerous, the importance of the cascading problem was again recognized. Several schemes particularly adapted to this method were devised to analyze and correct for cascading effects, and it has become standard practice to apply such procedures in beam-foil measurements.[2]

Nevertheless, two recent comprehensive comparisons between beam-foil lifetime data and theoretical results[3,4] show consistent slight systematic discrepancies in the direction that could be caused by cascading. While it is not certain that the aforementioned discrepancies will find their explanation in such effects, cascading is a prime suspect at this time.

For the detailed analysis of this effect, it is very useful to construct beam-foil decays synthetically from accurate theoretical data for simulated experimental conditions. Of particular interest are the questions whether customary cascade analysis—i.e., a fit to two or three exponential terms representing the primary decay, the principal cascades, and a constant background—is a sufficiently accurate correction, and whether a decay which seems to be single exponential for the main part of a curve might actually be the result of several contributing cascades. It is furthermore of interest to find some general answers to the question of cascading effects in beam-foil experiments, and to find reasons why they seem to be much more severe for some transitions and species than for others.

Such an analysis appears to be possible by assessing atomic energy-level and lifetime distributions as a function of atomic structure, particularly as a function of principal quantum number, and by taking the specific beam-foil population mechanism into account.

In this paper, we report on such an analysis of cascading effects in beam-foil spectroscopy. We have found indications that the cascading problem becomes progressively more serious for heavier ions. We have therefore taken the $4s$-$4p$ resonance line of three ions of the copper isoelectronic sequence as a specific example. By utilizing atomic-structure theory and the results of recent simulation studies on the sodium and beryllium sequences,[5,6] we arrive at conclusions of general interest. Specifically, we shall show that situations exist for $\Delta n = 0$ transitions where the radiative decay deceptively appears to be that of a single exponential for the principal part of the decay curve, but where significant cascading actually is present,

affecting the value of the apparent lifetime. Furthermore, we shall show that accurate beam-foil results are difficult to obtain for these $\Delta n = 0$ transitions, if the cascade analysis is limited to the widely used multiexponential fitting techniques.

II. CASCADE MODELING

We assume in the following that the decay of an excited atomic level occurs purely by spontaneous emission, i.e., that collisional depopulation and repopulation as well as radiation trapping (self-absorption) and induced emission are negligible. For the very low densities of ion beams in beam-foil experiments this is a realistic assumption.

The intensity of radiation due to a spontaneous transition of electrons from a higher atomic energy level p to a lower level q is given by

$$I_{pq}(t) = N_p(t) A_{pq} h\nu_{pq}, \tag{1}$$

where $N_p(t)$ is the population of level p at time t expressed as the number of atoms in state p per unit volume element, A_{pq} is the transition probability per unit time, and ν_{pq} is the transition frequency.

If energy levels lying above p are also excited, and if these levels spontaneously decay to p, then such transitions will serve to repopulate p, causing a longer effective decay time than would otherwise be observed (Fig. 1). Such repopulating transitions may take place through any number of intermediate states and by any radiative mechanism, e.g., electric dipole, electric quadrupole, magnetic dipole, etc. There may also be the possibility of the level p decaying to a state other than the one corresponding to the transition under study. The radiation intensity for the primary transition $p \rightarrow q$ is then still given by (1), but with a different $N_p(t)$ to reflect the effects of cascading. The equation governing $N_p(t)$ is

$$\frac{dN_p}{dt} = -N_p(t)\sum_{q=1}^{p-1} A_{pq} + \sum_{i=p+1}^{\infty} N_i(t) A_{ip}, \tag{2}$$

where the first term represents the depletion of the population of p by all allowed transitions to lower levels, and the second term accounts for repopulation due to the cascades. Similar equations must be written for each excited state $i = p+1, \ldots, \infty$ in order to obtain *its* population. The result is a system of coupled first-order differential equations in the variable t. $N_p(t)$ is easily solved for by using a diagrammatic technique developed by Curtis,[7] which conveniently groups cascading processes according to increasing orders of complexity. Utilizing this technique (for further details see Ref. 7), the following results for $N_p(t)$ are obtained:

For the *primary decay*, i.e., the decay of the level whose lifetime is being measured exclusive of any repopulating cascade effects, one obtains

$$P(t) = N_p(t=0) e^{-\alpha_p t}, \tag{3}$$

where $\alpha_j \equiv (\tau_j)^{-1} = \sum_{q=1}^{j-1} A_{jq}$ is the decay constant or inverse mean lifetime associated with the level j, and $N_i(0)$ is the population of the level i immediately after it leaves the foil. We will consider both of these quantities at length below.

A *first-order Rydberg cascade* involves the decay of an excited state i directly to state p with no intermediate steps:

$$C_i^{(1)}(t) = N_i(t=0) A_{ip} \left(\frac{e^{-\alpha_i t}}{\alpha_p - \alpha_i} + \frac{e^{-\alpha_p t}}{\alpha_i - \alpha_p} \right). \tag{4}$$

If all such cascades are added to the primary decay, the resulting equation for $N_p(t)$ is

$$N_p(t) = P(t) + \sum_{i=p+1}^{\infty} C_i^{(1)}(t). \tag{5}$$

The sum extends up through the members of a Rydberg series—hence the name "Rydberg cascade" is introduced.

In a *second-order Rydberg cascade*, an excited level j decays to an intermediate state i, followed by the decay of i to p, both decays taking place with no additional steps:

$$C_{ji}^{(2)}(t) = N_j(t=0) A_{ji} A_{ip} \times \left(\frac{e^{-\alpha_j t}}{(\alpha_p - \alpha_j)(\alpha_i - \alpha_j)} + \frac{e^{-\alpha_i t}}{(\alpha_p - \alpha_i)(\alpha_j - \alpha_i)} + \frac{e^{-\alpha_p t}}{(\alpha_i - \alpha_p)(\alpha_j - \alpha_p)} \right). \tag{6}$$

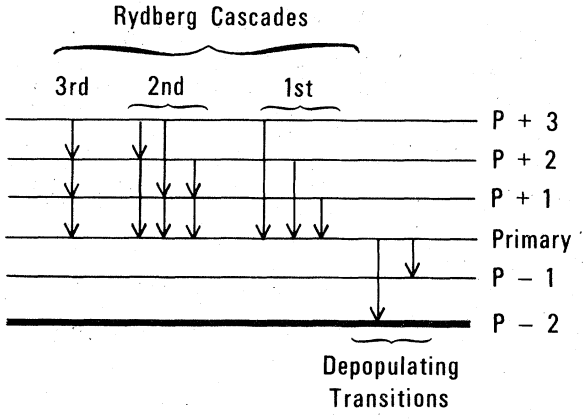

FIG. 1. Schematic energy-level diagram illustrating the radiative depopulation and repopulation of the primary level p. Repopulation is limited to three cascading levels $p+1$, $p+2$, $p+3$ and no consideration has been given to radiative selection rules which may cause some of the indicated decays to be very weak.

The decay equation including second-order Rydberg cascades is

$$N_p(t) = P(t) + \sum_{i=p+1}^{\infty} C_i^{(1)}(t) + \sum_{\substack{i=p+1 \\ j>i}}^{\infty} C_{ji}^{(2)}(t) . \tag{7}$$

We may generalize to an nth-order Rydberg cascade where an excited level k decays to an intermediate level j, followed by the decay of j to i, etc., until p is finally reached by a total of n transitions between k and p.

Finally, we follow Crossley *et al.*[5] in singling out the so-called "yrast" cascade, a special cascade which involves only levels with $n - l = 1$. Such cascades are particularly important in modeling the decay due to the large transition probabilities involved. The yrast decay chain is

$$\cdots \rightarrow 8k \rightarrow 7i \rightarrow 6h \rightarrow 5g \rightarrow \cdots .$$

When a level such as $4p$ is considered for a four-row atom, it is convenient to include in the yrast category the transitions $4f \rightarrow 4d \rightarrow 4p$, which constitute the only possible decay chain of these levels. The yrast contribution to the decay equation is

$$C_y^{(n)}(t) = N_n(t=0)\left(\prod_{i=p+1}^{n} A_{i,i-1}\right) \times \sum_{k=p+1}^{n} \frac{e^{-\alpha_k t}}{\prod_{\substack{j=p \\ (j\neq k)}}^{n} (\alpha_j - \alpha_k)} , \tag{8}$$

with n being the highest level in the sequence. If this distinction is made, one must be careful to exclude yrast decays when summing over Rydberg cascades, so that the same contribution is not counted twice.

When the contributions from all cascades are summed, the result is an expression describing the decay of level p in the presence of cascades from higher levels:

$$N_p(t) = P(t) + \sum_{i=p+1}^{\infty} C_i^{(1)}(t) + \sum_{\substack{i=p+1 \\ j>i}}^{\infty} C_{ji}^{(2)}(t) + \cdots + \sum_{i=p+1}^{\infty} C_y^{(i)}(t) . \tag{9}$$

In order to apply Eqs. (3)–(9) to model the radiative decay of an excited atomic energy level, it is necessary to have available the initial populations $N_i(t=0)$ of all cascading levels, or at least their relative distributions, as well as the transition probabilities linking them. We shall now turn to these topics.

III. INITIAL POPULATIONS

In order to use Eq. (9) to obtain N_p [and thus according to Eq. (1) the intensity of the emitted radiation], it is necessary to estimate the relative initial populations of atomic energy levels after beam-foil excitation, i.e., their relative populations at the time the ions leave the foil. In contrast to the situation for transition probabilities, the distribution of the initial populations among the excited states of the ion is poorly known, with no generally accepted universal model available.

Theoretically, the analysis of the motion of a complex ion through a foil is a difficult problem. Because of the small interatomic separation in solids, many of the outer electrons may be stripped off and reattached during the motion of the ion through the foil. Bickel *et al.*[8] point out that as the ion interacts with the foil electrons and nuclei it undergoes a continual series of excitations, ionizations, and recombinations. The dominant influence on the population distributions in beam-foil experiments appears therefore to be the interaction of the ions with the final layers of the foil. The exact mechanism of the population is not understood, but is expected to be some form of nonradiative electron capture from the electron cloud at the foil surface.

Trubnikov and Yavlinskii[9] have calculated the probability that an electron will be found in an excited $l = 0$ state of a hydrogen atom following the passage of a proton through a metal foil, finding for that special case

$$N_{n,l=0} \approx n^{-3} , \tag{10}$$

where n is the principal quantum number. McLelland[10] has shown that the situation is similar for a nonmetallic foil. A number of theoretical studies have been made for the case of protons or other light nuclei colliding with free atoms, resulting in power laws with a variety of exponents. Bates and Dalgarno[11] found for the case of protons incident on hydrogen atoms that the charge-exchange probability depends on the energy as well as the quantum numbers of the excited state. Hiskes[12] has shown that the process also depends on the target material. Finally, Dmitriev *et al.*[13] have indicated that the population distribution may also depend on the charge of the incident ion, with $Z \geq 4$ projectiles being populated mainly in excited states.

Experimental investigations of the beam-foil interaction have concentrated on light ions, with only a few studies available for $Z \geq 10$. For most ions, an n^{-a} dependence has been observed, although the exponents vary substantially. Dynefors *et al.*[14] have observed He I states up to $n = 11$, obtaining $a = 3$ except for small n.

The population of the angular momentum states within a given n is even less well understood, and is the major source of uncertainty in the estima-

tion of accurate initial populations. Observations by Bromander[15] and Davidson[16] indicate a statistical distribution according to L and S,

$$N \sim (2L+1)(2S+1), \tag{11}$$

for sufficiently high n, resulting in proportionately greater populations for high-angular-momentum states. Other experiments,[17-19] on hydrogen, point toward a trend in the opposite direction, i.e., smaller populations for high l states. In light ions, odd parity states have been found to be overpopulated with respect to even parity states.[14,16,20]

For the few experiments where the initial populations of heavy ions were studied—the case relevant to this work—the situation has been found to be quite different. In observations of transitions involving highly excited states of iron ions, Lennard and Cocke[21] found yrast transitions to be generally much stronger than other lines, indicating that the populations of these states may increase even *faster* than $(2l+1)$. In an earlier paper, Lennard *et al.*[22] point out that the intensity of lines from highly excited levels is surprising if a population distribution according to n^{-3} is assumed. Hallin *et al.*[24] have found that in Cl ions the intensities of yrast transitions *increase* with increasing principal quantum number, reach a maximum, and only then decline. This phenomenon has also been observed in NVII by Dufay *et al.*[23] Some of this increase may be due to cascade effects from higher states; if this is the case, however, even more severe cascade effects may be expected for lower lying primary states.

The above-cited observations and theoretical studies suggest not one, but a number of population distribution models as plausible. We have therefore taken the following simple models into consideration:

$$\begin{aligned}
&N_{nl} \sim n^{*-3} \quad \text{(model I)},\\
&N_{nl} \sim (2l+1)n^{*-4} \quad \text{(model II)},\\
&N_{nl} \sim (2l+1)n^{*-3} \quad \text{(model III)},\\
&N_{nl} \sim (2l+1)n^{*-3}\\
&\qquad \text{(yrast states only, model IV)},\\
&N_{nl} \sim (2l+1)n^{*-2} \quad \text{(model V)}.
\end{aligned} \tag{12}$$

Here $n^* = n - \delta$ (where δ is the quantum defect) has replaced n in the power law to better approximate the many-electron case. The first model represents a severe underpopulation of the upper yrast states and seems inconsistent with the heavy-ion experimental data; it may be considered to represent a lower limit to the cascade-state population. In model II, the exponent is further decreased while a statistical distribution with respect to l is provided. For large n and l, model II approaches model I:

$$(2l+1)n^{-4} \xrightarrow[l \to n-1]{} (2n-1)n^{-4} \approx 2/n^3 \quad \text{for large } n. \tag{13}$$

Model III appears to be the one most consistent with the experimental results of Lennard and Cocke,[21] Bromander,[15] Dufay *et al.*,[23] and others. Model IV is similar to model III except that only the yrast states are assumed to be populated. The last model features the largest populations of the cascade states.

It should be noted that none of these models account for the peaking of the population distributions at a given n, as observed by Hallin *et al.*[24] and Dufay *et al.*[23]

While the populations of models III and V are mathematically divergent, cutoffs in the population distribution will occur at some finite n, since large electron orbits do not exist in the beam due to the perturbing electric microfields of neighboring ions.

In the present calculations, we require only the initial populations relative to the $4p$ primary level, since each point in the decay curve is proportional to N_{nl}/N_{4p}. The relative populations for the models described above are

$$\begin{aligned}
N_{nl}/N_{4p} &= (n^*_{4p}/n^*)^3 \quad \text{(model I)},\\
&= \tfrac{1}{3}(2l+1)(n^*_{4p}/n^*)^4 \quad \text{(model II)},\\
&= \tfrac{1}{3}(2l+1)(n^*_{4p}/n^*)^3 \quad \text{(model III)},\\
&= \tfrac{1}{3}(2l+1)(n^*_{4p}/n^*)^3 \quad \text{(yrast only, model IV)},\\
&= \tfrac{1}{3}(2l+1)(n^*_{4p}/n^*)^2 \quad \text{(model V)}.
\end{aligned} \tag{14}$$

An interesting general observation regarding the contribution of high-level cascading to the decay of the primary level may now be drawn: For light ions with ground states $n=1$ or $n=2$, the initial populations of higher excited states relative to the ground state decrease rapidly with increasing n. For heavier ions with many electrons, however, where the lowest n is equal to 3, 4, or even 5, the decrease is much slower, so that even highly excited states may be expected to be appreciably populated and contribute to the cascading.

IV. TRANSITION PROBABILITIES

In order to apply the equations of Sec. II to the modeling of the decay curve of a state p, it is necessary to have available the atomic transition probabilities for all downward transitions involving each cascading level, as well as one for the primary level p. The accurate calculation of A values is known to be a difficult problem due to

their sensitivity to the wave functions involved. For the purposes of modeling decay curves, the transition probabilities determining the decay of the primary level have to be of especially high accuracy. Less accurate, more manageable computational methods such as the frozen-core Hartree-Fock approximation, the Coulomb approximation, even scaled hydrogenic data in some cases, were found sufficiently accurate for the cascading transitions. All of these methods are most accurate for wave functions far removed from the ionic core, which is the case for most of the cascading levels. (Further details on the calculation of transition probabilities for the sample decays we consider are given in Sec. V.)

Several interesting properties of cascades may be deduced from the Z and n dependences of atomic transition probabilities (for transitions with fixed l).

To obtain the Z dependence of atomic quantities, the atomic Hamiltonian is transformed and scaled by a change in the radial variable $\rho = Zr$. Using the electrostatic repulsion of the electrons as the perturbation, perturbation theory yields series expansions for the energy and wave function[25] in the parameter $1/Z$.

Retaining only lowest-order contributions, one finds for A: (a) for $\Delta n = 0$ transitions,

$$A_Z \sim Z A_{(Z=1)}; \tag{15}$$

(b) for $\Delta n \neq 0$ transitions,

$$A_Z \sim Z^4 A_{(Z=1)} . \tag{16}$$

For $\Delta n = 0$ hydrogenic transitions (fine-structure lines), the line strength is given by[26]

$$S = \mathcal{S}\, \tfrac{9}{4} n^2 (n^2 - l^2), \tag{17}$$

with $\mathcal{S}$ being an angular factor and l the smaller of the angular momentum quantum numbers. Equation (17) indicates that the transition probability for $\Delta n = 0$ transitions *increases* with principal quantum number. Such an increase results not only from the large overlap between the wave functions but also because as n increases the maxima occur at larger radii, serving to increase the transition matrix element.

The n dependence of the transition probability for $\Delta n \neq 0$ transitions is not as simply described, but one can show[26] that the line strength S decreases quite rapidly with n within a Rydberg series. Physically, this is caused by the decreasing overlap between the two radial wave functions. Although the $(\Delta E)^3$ energy dependence of A partially balances the decrease in line strength, it is not strong enough to change the general decline in A with increasing Δn in a Rydberg series.

Two general observations may now be drawn concerning the Z dependence of cascade effects. As Z increases, the lifetimes of many of the long-lived cascades from highly excited states decrease relative to the primary $\Delta n = 0$ transition due to the above-discussed rapid growth in A for $\Delta n \neq 0$ transitions, causing them to shift inward toward the foil. At some stage of ionization along an isoelectronic sequence, usually fairly low, these long-lived cascades will have moved all the way in to that main part of the decay curve which is normally used for the lifetime determination. The curve will still appear approximately linear since the various lifetimes become comparable. Since numerous cascades now contribute to the initial decay region, however, the slope of that curve will be different—and always less steep—than that which would result if no cascades were present, making the extraction of primary lifetimes very difficult. The effects of cascading are expected to be most serious for highly charged heavy ions where fairly low-lying levels of appreciable population contribute to the main region of the decay curve where the lifetime is to be extracted. Furthermore, as one moves upward along a homologous family of atoms, the effects of cascading from highly excited states may be expected to become more severe as more cascading levels are strongly populated. An additional factor for heavy ions is the existence of core-excited bound states, which are discussed later.

V. THEORETICAL DECAY CURVE SIMULATION

Knowing the initial population distribution of excited atomic states and the radiative transition probabilities between them, it is possible to construct a curve representing the decay of an excited ionic level using completely theoretical data. In modeling a decay, we use Eq. (9) which determines the population of the level being studied and, hence, according to Eq. (1), the intensity of radiation emitted in its spontaneous decay. The effect of cascading may be conveniently evaluated by successively adding terms to the equation corresponding to higher excited states and/or more complex cascades, and noting the effect on the final curve. Also, deliberate variations of the population distribution and of individual A values are valuable to test the importance of any one cascade on the final curve.

As an example of the analysis outlined above, we have chosen the $4s\ ^2S$-$4p\ ^2P$ resonance transition of the Cu I isoelectronic sequence. Since this transition has been observed to follow LS coupling,[29] we have chosen to model the multiplet decay (obtained by adding the component intensities) rather than the $\frac{1}{2}$-$\frac{1}{2}$ or $\frac{1}{2}$-$\frac{2}{3}$ lines individually. We have concen-

trated on the Cu-sequence ions Kr VIII, and, to a lesser extent Ga III and Ge IV, for the following reasons: (a) for this transition substantial differences exist between beam-foil and theoretical data; (b) this is a case where, according to the earlier discussion in Sec. IV, cascading effects might not noticeably alter the *shape* of the initial part of the decay curve from that of a purely one-exponential decay; (c) this transition is one of the very important ones for thermonuclear-fusion-research diagnostics; and (d) for the ion Kr VIII a very extended beam-foil decay curve is available to test the earlier-listed population models.

We have also modeled the $4s^2$-$4s4p$ resonance transition of the Zn sequence for the ion Kr VII, and obtained results analogous to our Cu-sequence analysis. However, this modeling is more uncertain and is therefore not discussed further. The main problem arises from the doubly excited $3d^{10}4p^2$ levels which cascade directly into the level of interest, but for which we were unable to establish reasonably reliable values for the initial populations.

(i) Transition probability data. For the primary lifetimes of Ga III and Kr VIII, we have used the results of the configuration-interaction calculations of Froese-Fischer[27] and the many-body perturbation theory results of Younger,[28] both of which include relativistic corrections to the wavelengths. For wavelengths and transition probabilities involving levels with $4 \leq n \leq 7$, $0 \leq l \leq 3$, we have calculated frozen-core Hartree-Fock data. Yrast cascades with $n \geq 5$ were considered hydrogenlike, and thus scaled hydrogenic data were used. This appears to be a good approximation insofar as the $n - l = 1$ wave functions involved have a small overlap with the complex core. The cascading levels considered are shown in Fig. 2.

For Ge IV, the primary lifetime was interpolated from Froese-Fischer's and Younger's calculations for neighboring ions. Yrast decays with $n \geq 5$ were again considered hydrogenlike, and the remainder of the data was obtained from the Coulomb approximation.

(ii) Initial populations. In contrast to the fairly reliable transition-probability data, there exists no generally accepted model for the population of excited states of an ion following beam-foil excitation. We have therefore searched for a precise and detailed beam-foil decay curve for use as a standard to which decay curves constructed according to the models described above may be compared, the closest fit presumably yielding the best approximation to the actual initial population distribution. Among the experimental data for ions of the Cu sequence,[29-34] the extended curve of Druetta and Buchet[29] for the $4p\,^2P^o$ decay of Kr VIII is the only one presently available which is suited for this purpose.

The fit of the simulated decay to the experimental decay curve was performed in the following manner:

Normalization of the experimental curve was performed at $t = 0.48$ ns (1 mm from the foil), which is the beginning of the important "linear" portion of the decay. The experimental data were multiplied by a normalization factor

$$\eta = S'_{\text{sim}} / S'_{\text{DB}},$$

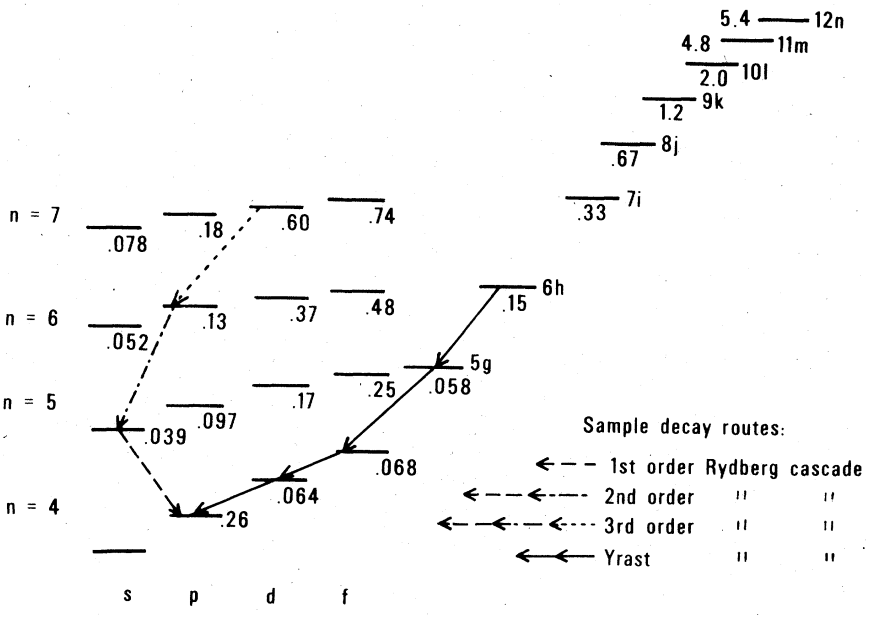

FIG. 2. Partial energy-level diagram of Kr VIII showing calculated mean lives, in ns, of the excited states used in simulating the primary decay, and samples of the different types of cascades.

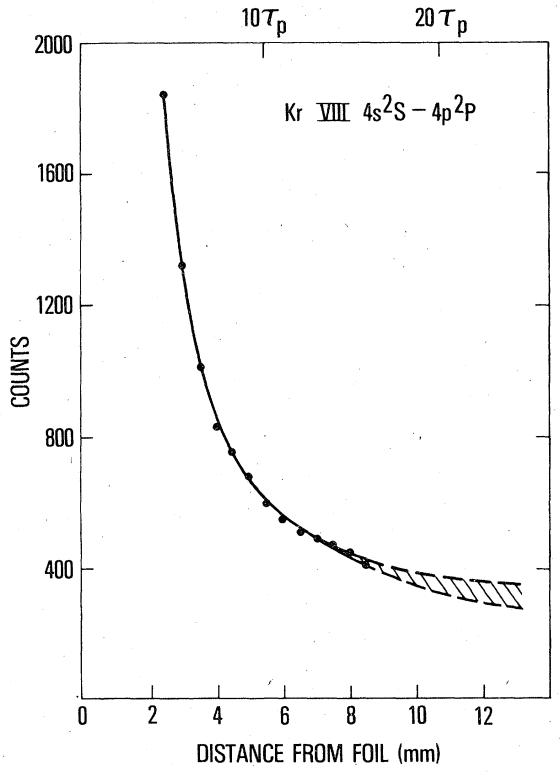

FIG. 3. Decay of the $4p\,^2P$ level of Kr VIII as observed by Druetta and Buchet (Ref. 29) on a linear scale. The intensities (photon counts) of the two lines comprising the multiplet have been summed to produce the present curve. The dashed area represents the extrapolation to the background.

where $S'_{\rm sim}$ is $N_{4p}(0.48)/N_{4p}(0)$ and $S'_{\rm DB}$ is the total photon count (or signal) of the Druetta and Buchet curve at $t = 0.48$ ns.

A residual constant background (e.g., due to scattered light) in the experimental curve was inferred from a linear plot of the (total) count, shown in Fig. 3, the estimated level being in the range 200–350 counts, or ~1% of the peak count. Therefore, a constant background has always been assumed, and its level has been treated as an adjustable parameter in our analysis, derived from the fit of the simulated decay curve. The "correct" population model should thus not only reproduce the shape of the experimental curve, but the approximate background count as well. Specifically, after normalization at $t = 0.48$ ns, the background count has been determined from a best fit between the normalized Druetta-Buchet curve and the simulated data in the range $t = 2.9$–3.6 ns (four points between 6.5 and 8.0 mm from the foil). With the total experimental count being the sum of signal and background

$$S_{\rm tot} = S_{\rm sig} + S_{\rm bg}, \tag{18}$$

(while the simulated curve represents the equivalent of a signal only), the normalized background count is found to be:

$$S_{\rm bg}^{\rm norm} = S_{\rm tot}^{\rm norm} - S_{\rm sig}^{\rm norm} = \eta S_{\rm DB} - S_{\rm sim}. \tag{19}$$

The individual background counts from the four points in the fitting region were averaged and the resulting approximate background correction applied to the complete experimental curve. Using an iteration process, the background-corrected experimental decay curve was then compared to the simulation and an evaluation of the population model was made. These comparisons will be discussed in Sec. VI.

After the initial background corrections were performed, it was found that by shifting the experimental curve with respect to the foil position by 0.5 mm ($t = 0.24$ ns) and repeating the above analysis, an even better fit could be obtained. Such a shift may not be unreasonable in light of the experimental uncertainties concerning the exact location of the foil. This shift in effect moves the origin of the experimental curve to the left by 0.5 mm.

VI. RESULTS AND DISCUSSION

Curves simulating the decay of the $4p\,^2P$ levels of Kr VIII assuming different population schemes are shown in Figs. 4–7. In Fig. 4, we compare simulations populated according to each of the

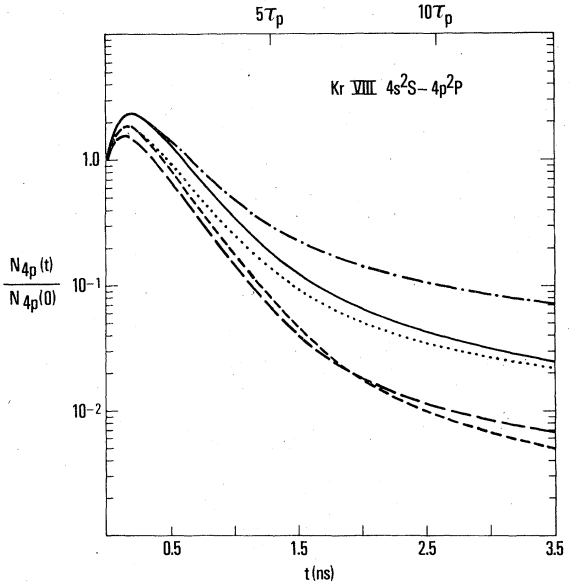

FIG. 4. Computer simulation of the decay of the $4p\,^2P$ level of Kr VIII corresponding to the five population models described in Sec. III: ----, model I; – – –, model II; —, model III; · · ·, model IV; – · – · –, model V.

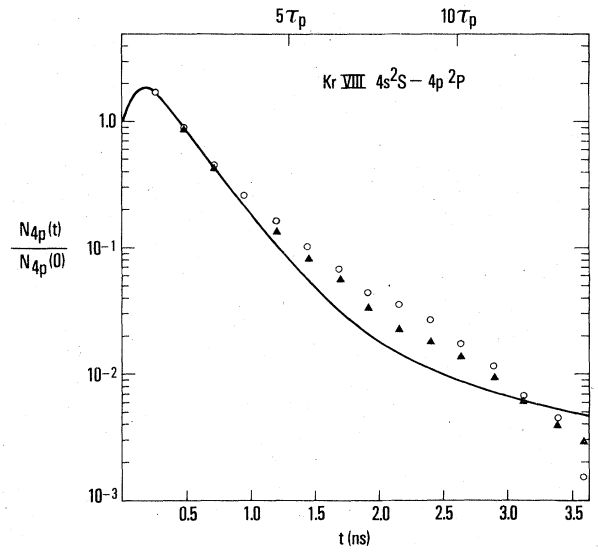

FIG. 5. Fit of the experimental decay curve of Druetta and Buchet to the computer simulation with population model I, described in the text (results for model II are very similar). The poor fit at long times indicates underpopulation of the cascade levels by this model. The circles are a direct plot of the experimental data on the given time (or distance) scale; the triangles are for an experimental curve where the foil position is assumed to be slightly shifted (by 0.5 mm or 0.24 ns in the time scale).

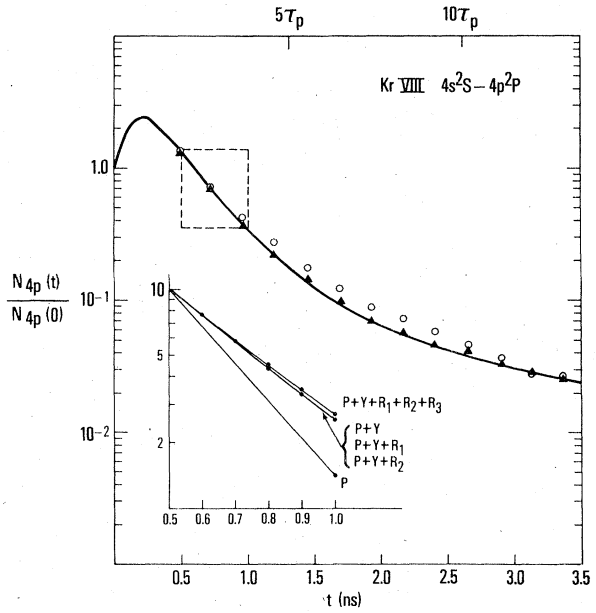

FIG. 6. Fit of the experimental decay curve of Druetta and Buchet to the computer simulation with population model III described in the text (results for model IV are very similar). The circles are a direct plot of the Druetta-Buchet data on the given time (or distance) scale. The triangles are for an experimental curve where the foil position is assumed to be shifted (by 0.5 mm or 0.24 ns in the time scale). The close agreement between simulated and experimental curves indicates that model III (or model IV) is close to the actual excited-state population distribution of the ion. The insert is an enlargement of the boxed region representing the important initial part of the decay, which shows the relative contributions of the various cascades included. P denotes primary, $P+Y$ denotes primary+all yrast cascades, $P+Y+R_1$ denotes primary+yrast + (first-order Rydberg cascades), etc. The dominant influence of the yrast cascades is clearly apparent.

models described in Sec. III. Pronounced differences in the curves are observed, and, after several primary lifetimes, the decay is in each case almost entirely governed by long-lived cascades. Inspection of the individual cascade contributions shows that the curves are not simply superpositions of a primary and one or two dominant cascades but that, depending on the point in time, there may be ten or more cascades, practically all of them "yrast," of comparable magnitude (but with different lifetimes) which combine in the decay. Furthermore, we have found that the relative importance of different cascades changes with time, e.g., a cascade which is important at $t = 1.5\tau_p$ may not affect the decay at $t = 5\tau_p$. Each cascade contributes most strongly in a specific portion of the curve, a factor which makes accurate cascade analysis quite difficult in that all portions of the decay curve are important in the fitting process.

In Figs. 5 and 6, we have used the detailed Kr VIII decay curve of Druetta and Buchet for tests of the various population models. For model I given in Sec. III, illustrated in Fig. 5, poor agreement is obtained between the best possible fit of the experimental data and the simulated curve. The background counts required to produce these fits (≈450) were practically equal to the total counts in the range where the fitting was carried out (6.5–8 mm from foil) and thus are inconsistent with the background extrapolation to long times, as shown in Fig. 3. Model II approaches model I at long times and thus suffers from the same difficulty in fitting the experimental data. It was not possible to fit the experimental data to model V, which overpopulates the cascade levels to such an extent that a negative background count would be required. We therefore conclude that population models I and II underestimate and that model V overestimates the actual initial population distribution of the ion.

In Fig. 6 we have compared the data of Druetta and Buchet with a decay curve simulation for Kr VIII based on population model III, including 20 yrast cascades, and all first-, second-, and third-

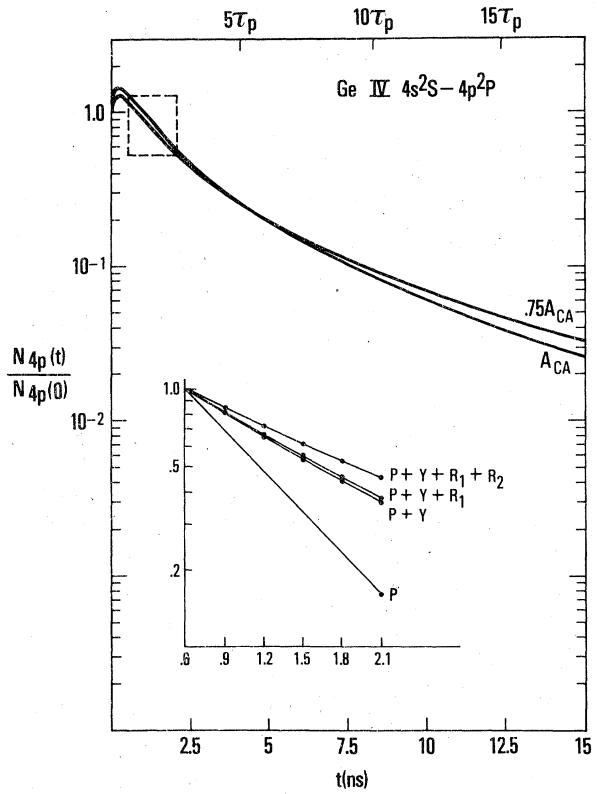

FIG. 7. Computer simulation of the decay of the $4p\ ^2P$ level of Ge IV constructed according to population model III but with different cascade lifetimes. In both cases the cascade lifetimes are from the Coulomb approximation (CA), but in one case they have been reduced by 25% to illustrate the insensitivity of the simulation to the exact values of the cascade lifetimes. The insert is an enlargement of the boxed area showing the relative contributions of the various cascades added to the A_{CA} curve.

order Rydberg cascades with $n \leq 7$ and $l \leq 3$ (a total of 30 exponentials). The experimental data were fitted with and without the 0.5-mm foil shift described above and with background counts of 350 and 230, respectively. These counts fall into the background range of 200–350 counts derived from the extrapolation (Fig. 3). While the unshifted curve is in reasonable agreement with the simulation (aside from a deviation in the intermediate region), the shifted curve is essentially an exact fit over the entire range. In both cases, there is good agreement between the slopes of the simulated and experimental curves in the initial "linear" region, as well as far from the foil. The ability to begin with entirely theoretical data and construct from it a decay closely matching an experimental curve is a strong indication that population model III is close to the actual case.

The insert to Fig. 6 details the contributions of the various cascades for the important initial decay region. Although the final curve appears deceptively single exponential, it is clear that significant cascading is occurring. So many exponentials are involved in the decay that a smoothing occurs, resulting in a straight line on a semilog plot, but with a slope for the final curve substantially different from that of the primary. In effect, the primary is "masked" by numerous cascades contained mainly in the yrast chain (see the near identity of $P+Y$, $P+Y+R_1$, and $P+Y+R_1+R_2$ in Fig. 6) and cannot be recovered by multiexponential analysis unless the exact nature of the masking is known. Since the simulated curves are in such good agreement with the experimental data of Druetta and Buchet, and since the yrast cascade lifetimes are reasonably well known, it is likely that such masking is occurring in the experiment as well.

For population case III, in which the experimental decay curve is so well simulated, we have applied to the simulated decay a cascade analysis similar to that which is customarily made on experimental data, namely a two-exponential fit with both coefficients and exponents as variables. As expected, and as seen in Table I, the resulting cascade-corrected primary lifetime is in good agreement with the beam-foil data of Refs. 29, 32, 33, and 34, *but not with the theoretical lifetime* for the $4p$ state which was actually used in constructing the curve. In other words, it was not possible to extract from the simulated decay curve the primary lifetime used in constructing it. This inability to extract *post facto* the primary lifetime arises because one is attempting to fit a curve made up of many exponentials with only two or three. Furthermore, there exist cascade terms which are important only for the approxi-

TABLE I. Comparison of experimental, simulated and theoretical lifetimes for the $4p$ level of Kr VIII. Both the experimental and simulated lifetimes are obtained by applying standard cascade analysis, i.e., a two-exponential fit to the decay curve. Numbers in parentheses indicate the cascade lifetime obtained from standard cascade analysis.

Beam foil (ns)	This simulation (ns)	Theory (ns)
0.36 (4.7)[a]	0.35 (2.8)	0.26[b]
0.39[c]		0.25[d]
0.35[e]		
0.35[f]		

[a] Reference 29.
[b] Reference 27.
[c] Reference 32.
[d] Reference 28.
[e] Reference 33.
[f] Reference 34.

mately "linear" region of the curve, i.e., they have no significant component either in the growing-in or growing-out portions of the curve, making their inclusion in a cascade analysis difficult. In all cases we have studied, the often applied replenishment ratio[35] is quite small, although there is appreciable cascading present.

We should note that we were able to extract the true simulated primary lifetime using the method of arbitrarily normalized direct cascades (ANDC) by Curtis.[2] This recently developed method of cascade analysis does not involve fitting the decay curve to a limited number of exponentials, but requires the measurement of all important direct cascades into the primary level—a requirement which substantially increases the scope of a beam-foil experiment.

We have also investigated the sensitivity of the simulations to changes in the cascade lifetimes. In Fig. 7, we show a simulated decay curve for Ge IV constructed according to population model III. In the same figure we show a simulation of the Ge IV decay curve with the same populations, but with the transition probabilities of the cascades arbitrarily reduced by 25%. The similarity of the two curves illustrates the relative insensitivity of the simulation to the exact values of the cascade lifetimes. (The lifetime of the primary has remained the same in both curves.)

The analysis of the influence of the various types of cascades on the shape of the curve and the extracted primary lifetime, already illustrated for the initial part of the decay curve in the insert of Fig. 6, shows that by far the most important cascades are the yrast. This is shown for the overall decay curve in Fig. 8. It is seen that Rydberg cascades, while altering the absolute magnitude of the curve, have a much smaller effect on the shape and the lifetime extracted from it. Thus a fit of the Druetta-Buchet curve to population model IV, which is identical to model III except that only yrast cascase levels are populated, results in the same close agreement between simulation and experiment as model III. Since first-order Rydberg cascades each involve only one transition between the cascading level and the primary level (usually strong ones, with short lifetimes), their main effect occurs at fairly small decay times. The contributions of second-, third-, and higher-order Rydberg cascades at longer times are easily understood in terms of the lifetimes and decay schemes involved. Several states contributing to these cascades are not highly excited and thus have appreciable initial populations. The decay paths, however, are more complex, so that in addition to relatively fast decays from low-lying levels, some low cascade levels (such as the

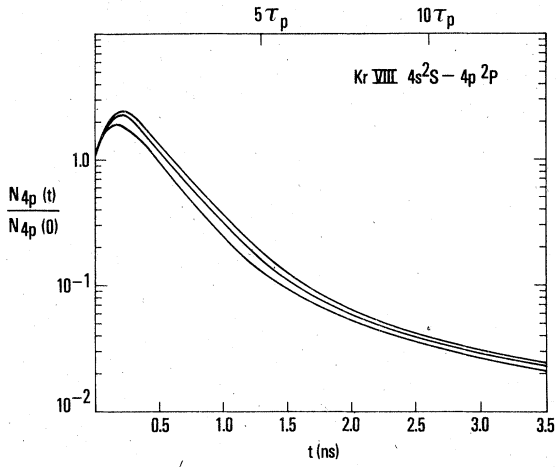

FIG. 8. Computer simulation of the decay of the $4p\ ^2P$ level of Kr VIII, showing the contributions of the various cascades for an extended range of the decay curve. The lowest curve includes the primary + yrast, the middle curve the primary + yrast + $R_1 + R_2$, and the topmost curve primary + yrast + $R_1 + R_2 + R_3$. The dominant influence of the yrast cascades at all times is clearly apparent.

$6f$ and $7f$ levels of Fig. 2) produce noticeable effects at longer times. Yrast cascades range from first order Rydberg-like to very extended decay chains and contribute strongly over the entire curve.

Another type of cascade, which does not directly follow the above classification, involves excitations of a core electron to levels such as $3d^9 4s\,4p$ and $3d^9 4p^2$ in the Cu sequence, which lie below the ionization limit. Such cascades are not present in lighter atoms without d electrons, and add an additional complication to the problem of extracting τ_p for heavy ions. Core excited states will not contribute to the Rydberg—or yrast—cascades, since they either directly connect to the $4p$ state (e.g., $3d^9 4p^2$) or to the ground state (e.g., $3d^9 4s\,4p$); or they are quasimetastable (e.g., $3d^9 4s^2$). The first decay possibility ($3d^9 4p^2$) could add a significant cascade. The other effects are indirect insofar as the core-excited levels are embedded in the single-electron Rydberg series and perturb the latter to various degrees. It was not possible to include these effects in our analysis, since very little is known about the positions of such states and their lifetimes.

It should be noted that Pinnington *et al.*[30] have recently measured the lifetime of the $4p$ state of Br VII and have performed a very limited cascade simulation to support their conclusion that there is little cascading influencing the decay curve. Their results are not inconsistent with ours, however, since very few of the important yrast cascades were included in their analysis. With a more extensive analysis, their results should be-

come quite similar to our own. It is one of the key conclusions of this study that such a detailed analysis, including Rydberg and yrast cascades to high orders, is necessary in order to determine what decays are most important in the simulation of a decay curve.

VII. CONCLUSIONS

Atomic decay curves simulating beam-foil excitation have been constructed from purely theoretical data for the $4s$-$4p$ transition of three ions of the copper sequence. The two principal requirements for the decay curve simulation are reliable transition-probability data connecting all pertinent atomic states, and a reliable model for the initial population distribution over the states.

For the particular case considered here (as well as many others), accurate transition-probability data are either available or can be readily calculated for transitions between higher-lying levels. The second requirement, knowledge of the initial population distribution, presents the major problem in simulating decays. The limited experimental evidence available on initial populations indicates complex dependences on ionic charge, the number of electrons in the ion, as well as the principal and angular quantum numbers of the particular excited state. While most studies of initial populations have concentrated on hydrogen[17-19] and helium,[14,16,20] the results of Lennard *et al.*[22] and others[21,23] indicate quite a different behavior for heavy ions such as chlorine or iron. It appears that the yrast states, important from the standpoint of cascading, are strongly populated in the beam-foil process. We have considered a number of plausible population models based on experimental observations, and have evaluated them by comparing the resulting simulations with the accurate and detailed experimental curve of Druetta and Buchet[29] for Kr VIII. With reliable transition probabilities, the goodness of the fit to the experimental curve is a measure of the accuracy of the population model. We were able to achieve excellent agreement between the two using the model $N_{n_l} \sim (2l+1)n^{*-3}$, which is also quite consistent with the above mentioned observations of strongly populated yrast states.[21-23]

One of the most important results of the present work is that one is unable to recover from the decay curve, by exponential-fitting methods, the actual primary lifetime used in its construction. The effect of cascading is to mask the true primary lifetime to such an extent that a decomposition of the curve, shaped significantly by at least ten components, into two or three exponentials is insufficient to remove the cascade changes. The primary lifetime extracted from our simulated curve by exponential fitting is, however, in good agreement with the quoted experimental values. This is an indication that the cascading problems causing the true lifetime to be masked in the simulations, should also be present in the experiments, and that this may be an explanation for the systematic discrepancy between theory and experiment discussed above.

In all our simulations we have found that the initial part of the decay curve is practically linear, although heavy cascading is taking place. Thus cascade effects do not become *apparent* until several primary lifetimes have elapsed. It is important for this reason that experimental decay curves should be recorded for at least 10 primary lifetimes.

The replenishment ratio in our simulations is always quite small, despite heavy cascading. This is not surprising, in that this parameter is based on the decomposition of the decay curve into only a few exponentials, which is certainly not valid in the present work. Since it is probable that cascade effects similar to those in our simulations also occur in experimental decays, the value of the replenishment ratio as a measure of the severity of cascading appears to be doubtful when based on the parameters of two- or three-exponential fit. On the other hand, beam-foil results obtained from few-exponential fits of decay curves may be highly accurate if no other excited states with lifetimes in the range of the primary level are appreciably populated. This situation is encountered for levels in very light ions. For levels involving resonance ($\Delta n = 0$) transitions the cascade situation becomes quite complex for third-row and heavier-element isoelectronic sequences. The abundance of in-shell and other low-lying levels grows with the addition of d levels, f levels, etc., and increasing numbers of doubly excited bound states appear in the spectra below the ionization limit. Furthermore, within the isoelectronic sequences themselves the cascading effects for $\Delta n = 0$ resonance transitions should become progressively more serious with increasing Z, because of the different Z scaling of the transition probabilities for cascade transitions.

The present study thus offers an explanation for the systematic discrepancies between beam-foil results (obtained by the customary exponential fitting of the decay curve) and advanced theoretical calculations that exist for the resonance transitions of ions in several heavy isoelectronic sequences. For alkali-metal-like isoelectronic sequences, very good agreement has been reported for the Li sequence[36] (where initial populations of significant cascade states are small), but there

exists a (10–15)% discrepancy for the Na sequence,[5] and a 30% discrepancy for the Cu sequence.[37] Recent theoretical studies on the Zn sequence by Weiss[38] and Shorer and Dalgarno,[39] and on the Au sequence by Migdalek[40] indicate continued serious disagreement for still heavier isoelectronic sequences.

While it is possible to apply an extensive cascade-analysis technique which could extract accurate primary lifetimes, perhaps by a combination of experiment and cascade simulation, such a technique would be vastly more complex than the customary exponential-fitting procedure. A technique in this spirit is the ANDC method of Curtis,[2] which is based entirely on measured decay curves. Although this method of analysis comes at the expense of a considerably greater demand on the experimental technique, it points in the direction of future accurate beam-foil lifetime work.

ACKNOWLEDGMENTS

We would like to thank A. W. Weiss for many helpful discussions concerning this work. This work was supported in part by the U. S. Department of Energy.

[1]S. Heron, R. W. P. McWhirter, and E. H. Rhoderick, Proc. R. Soc. Lond. 234, 565 (1956).
[2]L. J. Curtis, *Beam Foil Spectroscopy* (Springer-Verlag, Berlin, 1976), edited by S. Bashkin, p. 63.
[3]E. H. Pinnington, A. E. Livingston, and J. A. Kernahan, Phys. Rev. A 8, 1004 (1974).
[4]C. Laughlin and A. Dalgarno, Phys. Rev. A 8, 39 (1973).
[5]R. J. S. Crossley, L. J. Curtis, and C. Froese-Fischer, Phys. Lett. A 57, 220 (1976).
[6]H. P. Mühlethaler and H. Nussbaumer, Astron. Astrophys. 11, 1 (1976).
[7]L. J. Curtis, Am. J. Phys. 36, 1123 (1968).
[8]W. S. Bickel, K. Jensen, C. S. Newton, and E. Veje, Nucl. Instrum. Methods 90, 309 (1970).
[9]B. A. Trubnikov and Yu. N. Yavlinskii, Zh. Eksp. Teor. Fiz. 52, 1638 (1968) [Sov. Phys. JETP 25, 1089 (1967)].
[10]G. J. McLelland, Ph.D thesis (University of Sydney, Sydney, Australia, 1968) (unpublished).
[11]D. R. Bates and A. Dalgarno, Proc. Phys. Soc. Lond. A 66, 972 (1953).
[12]J. R. Hiskes, Phys. Rev. 180, 146 (1969).
[13]I. S. Dmitriev, Ya. A. Teplova, and U. S. Nikolaev, Zh. Eksp. Teor. Fiz. 61, 1359 (1971) [Sov. Phys. JETP 34, 723 (1972)].
[14]B. Dynefors, I. Martinson, and E. Veje, Phys. Scr. 13, 308 (1976).
[15]J. Bromander, Nucl. Instrum. Methods 110, 11 (1973).
[16]J. Davidson, Phys. Rev. A 12, 1350 (1975).
[17]R. M. Schectman, Phys. Rev. A 12, 1717 (1975).
[18]R. Tielert and H. H. Bukow, Z. Phys. 264, 119 (1975).
[19]A. S. Goodman and D. J. Donahue, Phys. Rev. 141, 1 (1975).
[20]N. Andersen, G. W. Carriveau, A. F. Glinska, K. Jensen, J. Melskens, and E. Veje, J. Phys. 253, 53 (1972).
[21]W. N. Lennard and C. L. Cocke, Nucl. Instrum. Methods 110, 137 (1973).
[22]W. M. Lennard, R. M. Stills, and W. Whaling, Phys. Rev. 6, 884 (1972).
[23]M. Dufay, A. Davis, and J. Desequelles, Nucl. Instrum. Methods 90, 85 (1970).
[24]R. Hallin, J. Lindskog, A. Marelius, J. Pihl, and R. Sjödin, Phys. Scr. 8, 209 (1973).
[25]W. L. Wiese and A. W. Weiss, Phys. Rev. 175, 50 (1968).
[26]H. A. Bethe and E. E. Salpeter, *Quantum Mechanics of One and Two Electron Atoms* (Academic, New York, 1957).
[27]C. Froese-Fischer, J. Phys. B 10, 1241 (1977).
[28]S. M. Younger (to be published).
[29]M. Druetta and J. P. Buchet, J. Opt. Soc. Am. 66, 433 (1976).
[30]E. H. Pinnington, J. A. Kernahan, and K. E. Donnelly, J. Opt. Soc. Am. 67, 162 (1977).
[31]G. Sorensen, Phys. Rev. 7, 85 (1973).
[32]E. J. Knystautas and R. Drouin, J. Quant. Spectrosc. Radiat. Transfer 17, 551 (1977).
[33]A. E. Livingston, Ph.D. thesis (University of Alberta, Edmonton, Alberta, 1974) (unpublished).
[34]D. J. G. Irwin, J. A. Kernahan, E. H. Pinnington, and A. E. Livingston, J. Opt. Soc. Am. 66, 1396 (1976).
[35]L. J. Curtis, H. G. Berry, and J. Bromander, Phys. Scr. 2, 216 (1970).
[36]G. A. Martin and W. L. Wiese, J. Phys. Chem. Ref. Data 5, 537 (1976).
[37]W. L. Wiese and S. M. Younger, in *Beam Foil Spectroscopy*, edited by I. A. Sellin and D. J. Pegg (Plenum, New York, 1976).
[38]A W. Weiss unpublished.
[39]P. Shorer and A. Dalgarno, Phys. Rev. A 16, 1502 (1977).
[40]J. Migdalek, Can. J. Phys. 54, 2272 (1976).